

# On the sound field radiated by a tuning fork

Daniel A. Russell

Science and Mathematics Department, Kettering University, Flint, Michigan 48504

(Received 14 June 1999; accepted 25 April 2000)

When a sounding tuning fork is brought close to the ear, and rotated about its long axis, four distinct maxima and minima are heard. However, when the same tuning fork is rotated while being held at arm's length from the ear only two maxima and minima are heard. Misconceptions concerning this phenomenon are addressed and the fundamental mode of the fork is described in terms of a linear quadrupole source. Measured directivity patterns in the near field and far field of several forks agree very well with theoretical predictions for a linear quadrupole. Other modes of vibration are shown to radiate as dipole and lateral quadrupole sources. © 2000 American Association of Physics Teachers.

## I. INTRODUCTION

If one rotates a sounding tuning fork once about its long axis while holding the fork close to the ear, one finds four positions where the sound is loud, alternating with four positions where the sound is very quiet.<sup>1</sup> The loud regions are indicated as A and B in Fig. 1(b) and the quiet regions fall approximately along the dotted lines. By rotating the fork close to the end of a tuned resonance tube this phenomenon may be demonstrated to a group of people.<sup>2,3</sup> If one listens very carefully, one finds that maxima in the plane of the fork [regions A in Fig. 1(b)] are noticeably louder than those perpendicular to the fork (regions B).

A very different pattern of loud and quiet regions is heard, however, when a sounding tuning fork is held at arm's length from the ear and rotated once about its long axis. Now, only two maxima are heard, both in the plane of the fork (regions A), while minima are heard perpendicular to the fork (regions B). The differences between near- and far-field sound patterns may be effectively demonstrated to a larger audience by using an inexpensive microphone and preamp connected to an oscilloscope.

While several older acoustics texts describe the sound field radiated by a tuning fork,<sup>1-6</sup> discussion of this phenomenon is absent from recent acoustics texts. Unfortunately, those older texts which attempt to explain the sound field close to the fork do so in terms of constructive and destructive interference effects. This would seem an implausible explanation since the tines of a tuning fork are almost always separated by a distance much smaller than half a wavelength of the sound emitted, which means that interference effects should be noticed only at significant distances from the fork tines. Sillitto<sup>7</sup> has shown that close to the fork it is path-length-dependent amplitude differences which determine the sound field and that path-length-dependent phase differences only become dominant at large distances from the fork.

The goals of this paper are to address some of the misconceptions concerning the sound field radiated by a vibrating tuning fork, to discuss the quadrupole nature of the tuning fork sound field, and to present experimental measurements of the near-field and far-field radiated patterns. While primary attention will focus on the sound field produced by the principal mode of the tuning fork, as shown in Fig. 1(a), radiation patterns from other less frequently observed vibrational modes will also be discussed.

## II. THE TUNING FORK AS A LATERAL QUADRUPOLE

A typical explanation of the sound field produced by a tuning fork goes something as follows.<sup>2,3,5,8</sup>

When the tines move outward, a compression is sent out in the directions of A in Fig. 1(b) and simultaneously a rarefaction in the directions of B. As the tines move inward they send out a rarefaction in the directions of A and a compression in the directions of B. These sets of waves are always in opposite phase, and along the directions 45° from the plane of the tines (dotted lines) the compressions of one set of waves and the rarefactions of the other will coincide, and there will be silence.

As an example of a sound source which follows the above description, consider a cylinder whose radius alternately expands and contracts according to<sup>9</sup>

$$r(\theta, t) = R + \cos(2\theta)\sin(\omega t), \quad (1)$$

where  $R$  is the mean radius of the cylinder. Figure 2 shows one cycle of the radial oscillation of the cylinder. The cylinder simultaneously elongates in the horizontal direction, pushing air outward, and contracts in the vertical direction drawing air inward. Half a cycle later the cylinder contracts in the horizontal direction drawing air inward and expands in the vertical direction pushing air outward. Figure 3 shows two frames from an animation created with MATHEMATICA,<sup>10,11</sup> which shows the sound field resulting from Eq. (1). The animation is available as an animated GIF movie on the WWW.<sup>12</sup> The two still frames differ by one half-period of the cylinder motion. It is clear to see that waves propagating in the horizontal and vertical directions have opposite phase, and that the waves completely cancel along lines 45° from the horizontal.

A similar sound field is produced when four identical omnidirectional sources are placed in a lateral quadrupole arrangement as shown in Fig. 4(a). Such an arrangement of sources may be effectively demonstrated by passing a low frequency signal through four small boxed loudspeakers with opposite polarities.<sup>13</sup> The expression for the complex sound pressure amplitude produced by a lateral quadrupole may be derived as<sup>14,15</sup>

$$p(r, \theta) = \frac{A}{r} \left( \frac{3}{r^2} - k^2 - \frac{i3k}{r} \right) \sin \theta \cos \theta, \quad (2)$$

where  $A$  is an amplitude factor which depends on the size, strength, and frequency of the quadrupole source. The presence of the “ $i$ ” in the third term in parentheses indicates that

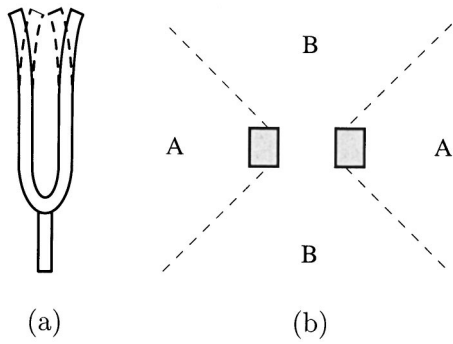


Fig. 1. (a) Principal mode of a tuning fork. (b) End view of a tuning fork showing regions of loud and quiet.

this term is  $90^\circ$  out of phase from the other terms. The variable  $k$  is the wave number ( $k = 2\pi/\lambda$ ) and  $r$  is the distance to the observer. The expression in Eq. (2) is valid for all distances  $r$ . At large distances  $r$  (termed the far field) the pressure amplitude may be approximated by

$$p(r, \theta) = \frac{Ak^2}{r} \sin \theta \cos \theta. \quad (3)$$

The angular dependence is the same for Eqs. (2) and (3). Moving from near field to far field has no effect on the angular dependence of the directivity pattern.

Figure 4(b) shows a polar plot of the directivity pattern for a lateral quadrupole source. For this and all following plots, the pressure amplitude is plotted on a logarithmic scale, with units of decibels. In addition, all plots have been normalized to the maximum value, as is the accepted practice for directivity plots.<sup>16</sup> The directivity plot shows that the lateral quadrupole pressure field exhibits four directions where sound is radiated very well alternating with four directions in which no sound is radiated. This directivity pattern matches nearly exactly the sound field predicted by the cylindrical source as shown in Fig. 3.

A lateral quadrupole source model has been used to describe the sound field of the tuning fork.<sup>3,8</sup> While this might appear to explain what one hears in the near field of a tuning fork, there are several problems. First, this model does not explain why one hears only two maxima and minima when the fork is held at arm's length from the ear. If the tuning fork behaved as a lateral quadrupole the sound field should be the same at any distance from the fork. Second, this model implies that close to the fork all four loud regions should be equally loud. However, close listening reveals that maxima in the plane of the fork are definitely louder than those perpendicular to the plane of the fork. Third, as the data will show, the minima do not fall exactly along  $45^\circ$  from the plane of the tines.

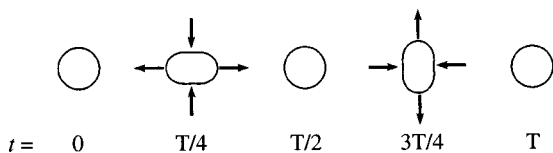


Fig. 2. The radial oscillation of a cylinder according to Eq. (1). Times are fractions of one period,  $T$ , of the motion.

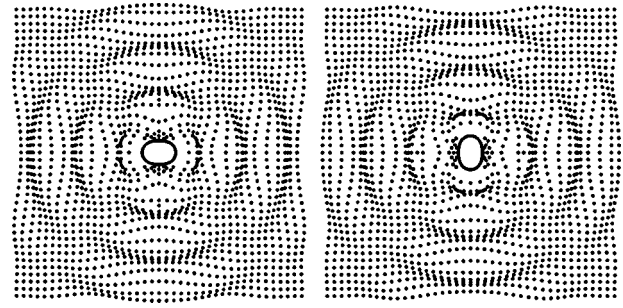


Fig. 3. Frames from an animated GIF movie (Ref. 12) animating the sound field produced by an oscillating cylinder according to Eq. (1).

### III. THE TUNING FORK AS A LINEAR QUADRUPOLE

When a tuning fork vibrates in its fundamental mode, the tines oscillate symmetrically in the plane of the fork, as shown in Fig. 1(a). Each individual tine might be modeled by a dipole source,<sup>17,18</sup> much like an un baffled loudspeaker<sup>19</sup> and a transversely oscillating sphere<sup>14</sup> are treated as a dipole sources. Dipole sources are discussed further in Sec. V.

A combination of two dipole sources with opposite phase, such that the dipole axes lie along the same line, is called a linear, or longitudinal quadrupole source. The source distribution for a linear quadrupole is shown in Fig. 5(a). The exact expression for the pressure field radiated by a linear quadrupole may be derived as<sup>14,15</sup>

$$p(r, \theta) = \frac{A}{r} \left[ (1 - 3 \cos^2 \theta) \left( \frac{ik}{r} - \frac{1}{r^2} + \frac{k^2}{3} \right) - \frac{k^2}{3} \right]. \quad (4)$$

The result by Sillitto<sup>7</sup> gives an equivalent expression in terms of Legendre polynomials and spherical Bessel functions. Figure 5(b) is a polar plot showing the directivity pattern for a longitudinal quadrupole with an observer distance  $r = 0.05$  m from a 426-Hz source, so that  $kr = 0.39$ . The product  $kr$  is typically used to define the boundary between the near field and far field of a source. As a general rule of thumb, if  $kr < 1$  the observer is in the near field, and if  $kr > 1$  the observer is in the far field.

The near-field directivity pattern in Fig. 5(b) matches what is heard close to a tuning fork. There are four maxima, two in the plane of the fork and two perpendicular. However, the maxima perpendicular to the plane of the fork (at  $90^\circ$  and  $270^\circ$ ) are approximately 5 dB lower than the maxima at  $0^\circ$  and  $180^\circ$ . Since changes in sound pressure level of 5 dB are clearly noticeable to the ear<sup>15</sup> this difference in amplitude is quite observable. Furthermore, the minima are not symmetric

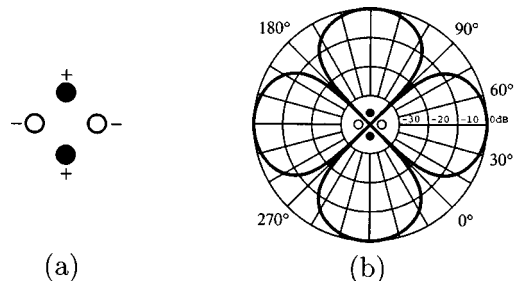


Fig. 4. Lateral quadrupole model for a tuning fork: (a) simple source arrangement; (b) directivity pattern.

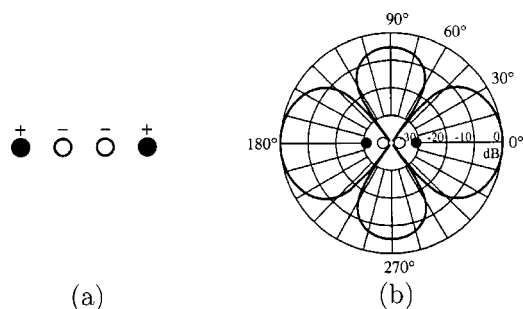


Fig. 5. Linear quadrupole: (a) simple source arrangement; (b) near-field directivity pattern for  $kr=0.39$ .

cally spaced at  $45^\circ$  from the plane of the fork as predicted by a lateral quadrupole model. Instead the first minima occurs at approximately  $54^\circ$ .

At large distances  $r$  such that  $kr \gg 1$  the exact expression in Eq. (4) approximates to

$$p(r, \theta) = \frac{Ak^2}{r} \cos^2 \theta. \quad (5)$$

Figure 6 compares the far-field directivity pattern calculated from the exact expression in Eq. (4) with the far-field approximation in Eq. (5). In Fig. 6(a) the observer distance is  $r=1$  m from a 426-Hz source ( $kr=7.8$ ). These plots show that in the far field of a linear quadrupole, only two maxima are present, with minima perpendicular to the plane of the fork. This matches what one observes when a tuning fork is held at arm's length from the ear.

Figure 7 shows a contour plot of the pressure field produced by a longitudinal quadrupole source. White represents the highest pressure and black the lowest pressure. The contour plot represents a  $100 \text{ cm} \times 100 \text{ cm}$  region with the source at the center of the plot; the two dipoles comprising the quadrupole, and representing the tuning fork tines, are at  $\pm 1$  cm aligned horizontally. The wavelength is 80.5 cm, corresponding to a frequency of 426 Hz (the speed of sound is taken to be 343 m/s). The pressure field shown corresponds to the time just after the tines have reached their maximum outward positions, thus producing a maximum pressure region in front of each tine in the horizontal directions.

The contour plot in Fig. 7 shows both the near-field and far-field behavior of the pressure field. An animated version is available on the WWW.<sup>12</sup> The animation is in color and shows the pressure field as the fork tines go through one

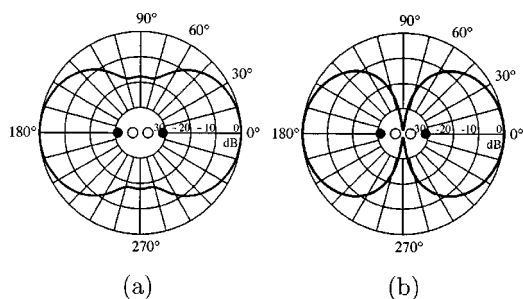


Fig. 6. Far-field directivity patterns for a linear quadrupole. (a) Exact expression from Eq. (4) with  $kr=7.8$ ; (b) far-field approximation from Eq. (5).

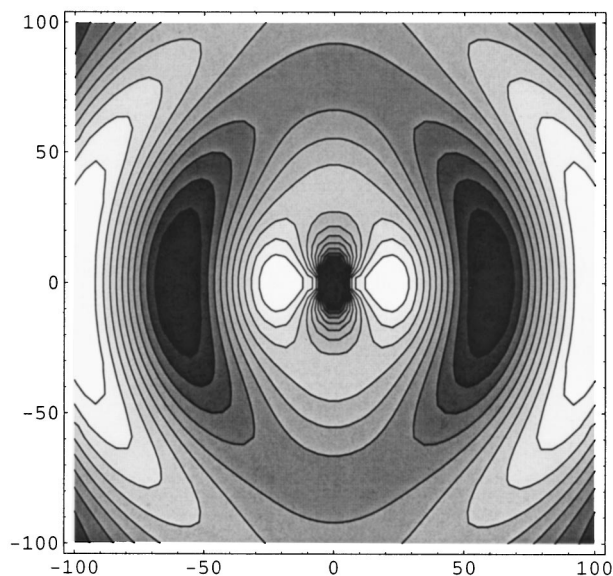


Fig. 7. Contour plot showing the pressure field produced by a longitudinal quadrupole. White represents the highest pressure and black represents the lowest pressure.

complete cycle of their motion. Readers are encouraged to view the animation to more clearly see the transition from near field to far field.

The contour plot and the animation show a significant wave front radiating away from the tines in the horizontal directions, as a result of the outer surface of the tines pushing on the air as they oscillate back and forth. A much weaker wave motion propagates in the vertical directions, with the amplitude decaying dramatically within the first 20 cm or so from the fork.

The transition from near field to far field is the result of a transition from path-length-dependent amplitude differences to path-length-dependent phase differences.<sup>7</sup> Consider the tuning fork as a linear quadrupole arrangement of four point sources, as in Fig. 5(a). When the observer location is very close to the center of the fork, along a vertical orientation, the distance to the inner pair of sources ( $-\circ$ ) is smaller than that to the outer pair ( $+\bullet$ ). Since the pressure from a point source decreases as  $1/r$  the pressure amplitude from the closer inner pair of sources dominates the near field and a significant negative pressure is observed perpendicular to the source alignment. As one moves in the vertical direction away from the sources, the path length differences to each source become negligible and the phase differences dominate. Since there are an equal number of positive and negative sources, the pressures effectively cancel and there is very little resultant vertically propagating wave motion in the far field. A similar behavior may be observed for the electric potential around an electric linear quadrupole source.<sup>20</sup>

#### IV. EXPERIMENTAL MEASUREMENTS

Measurements were made in the near and far fields of two different sized 426.6-Hz aluminum tuning forks and a 2000-Hz aluminum fork. Dimensions for each fork are shown in Table I. As shown in Fig. 8, a small NdFeB magnet was attached, with wax, to each tine at about  $3/4$  of the tine length from the top of the fork. An electromagnetic coil was placed over one magnet and driven by a sine wave generator

Table I. Dimensions of tuning forks used in experiment.

Fork frequency (Hz)	Tine length (cm)	Tine separation (cm)	Tine width (cm)	Tine thickness (cm)
426.6	13.04	2.14	0.89	1.29
426.6	12.17	1.67	0.72	0.94
2000	6.22	1.11	0.71	0.93

at the natural frequency of the loaded fork. The second magnet provided symmetric loading on the other tine. The fork was firmly clamped in a support and centered on a rotating turntable. Sound absorbing material was placed around the apparatus to reduce reflections from the table top and walls. A small Radio Shack electret microphone was mounted at a fixed distance from the center of the fork, at a height just below the top of the fork. The microphone output was displayed on a Stanford Research Systems model SR780 fast Fourier transform analyzer using units of sound pressure level (dB). The decibel level was measured every 5° as the fork was rotated about its long axis.

Figure 9 shows the measured directivity pattern (normalized to the level at 0°) at a distance of 5 cm from the small 426.6-Hz tuning fork. With the magnets attached, the fundamental frequency of the fork was lowered to 418.76 Hz so that  $kr=0.38$ . The orientation of the fork is shown in the figure by the two small rectangles at the center of the plot. Figure 9(a) attempts to fit the data with a lateral quadrupole directivity pattern using Eq. (2) while Fig. 9(b) attempts to fit the same data with a linear quadrupole directivity pattern using Eq. (4). While neither theoretical curve fits the data perfectly, the linear quadrupole curve (b) more closely matches the overall shape, and correctly predicts the 5-dB reduction at 90° and 270°. In addition, the linear quadrupole fit also more closely matches the angular location of the minima, the first of which falls at approximately 50°. Slight differences between theory and data should be expected since the theory is for four point sources arranged as a linear quadrupole, while the actual tuning fork is two rectangular bars oscillating back and forth. Still, the linear quadrupole fit is quite good, and much better than the lateral quadrupole fit.

At a distance of 20 cm from the small 426.6-Hz fork ( $kr=1.53$ ), the fit between measured levels and linear quadrupole theory is still quite good, as shown in Fig. 10(a). The fit is still good at a distance of 80 cm ( $kr=6.13$ ), which is approximately arm's length, in Fig. 10(b). While the theory and data do not agree exactly near 90° and 270°, the measured levels are more than 10 dB down from the levels in the

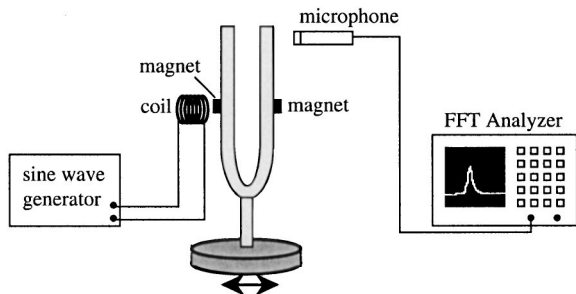


Fig. 8. Experimental apparatus for measuring the directivity pattern for sound radiation from a tuning fork.

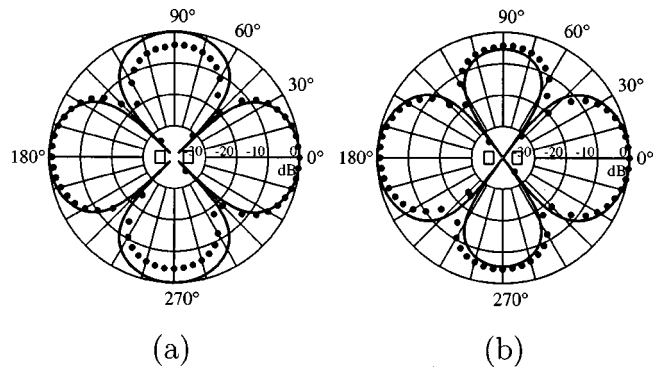


Fig. 9. Sound pressure level directivity patterns 5 cm from the small 426-Hz fork. (a) Data fit with lateral quadrupole from Eq. (2). (b) data fit with linear quadrupole from Eq. (4).

plane of the fork. Such a sound pattern would give the impression of two maxima in the plane of the fork and two minima perpendicular to the plane of the fork, as is observed when the fork is held at arm's length from the ear.

Figure 11 shows measurements for the 2000-Hz fork at distances of 4 and 78 cm. The loading of the magnet lowered the fundamental frequency to 1960 Hz so that  $kr=1.44$  and  $kr=28.0$ , respectively. Both the near-field and far-field measurements match the theoretical curves quite closely. In the near field there are four maxima and four minima. In the far field there are two maxima in the plane of the fork tines, while perpendicular to the tines the sound pressure level is approximately 5 dB lower. The near-field pattern for the 2000-Hz fork (4 cm  $\rightarrow kr=1.44$ ) looks very similar to the midfield directivity pattern for the 426.6-Hz fork (20 cm  $\rightarrow kr=1.53$ ), as should be expected since the values of  $kr$  are similar.

Agreement between measurements and theory for both near and far fields verifies that the tuning fork behaves as a linear quadrupole source when vibrating in its fundamental mode. A lateral quadrupole model, which is based on interference effects, does not match the measured sound fields.

## V. RADIATION FROM OTHER VIBRATIONAL MODES

While the fundamental mode of a vibrating tuning fork acts like a longitudinal quadrupole source, there are other

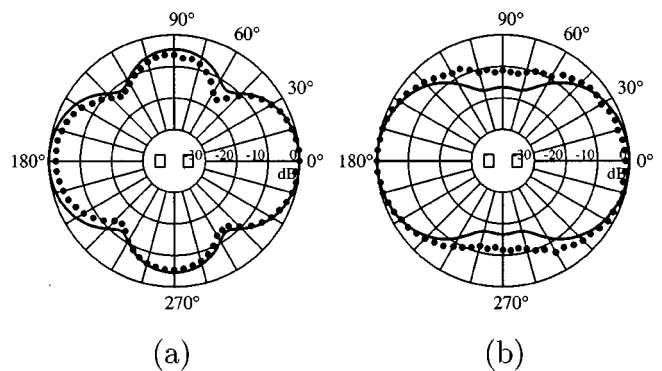


Fig. 10. Measured directivity patterns for the small 426-Hz fork at a distance of (a) 20 cm ( $kr=1.56$ ) and (b) 88 cm ( $kr=6.25$ ) from the center of the tines. The solid curve represents linear quadrupole theory and points represent data.

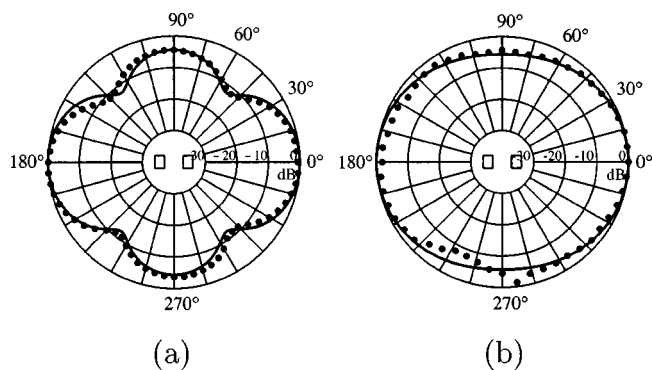


Fig. 11. Measured directivity patterns for the 2000-Hz fork at a distance of (a) 4 cm ( $kr=1.46$ ) and (b) 78 cm ( $kr=28.6$ ) from the center axis of a 2000-Hz tuning fork. The solid curve represents theory and points represent data.

modes of vibration which produce different directivity patterns. The second most familiar vibrational mode of a tuning fork is the “clang” mode, which occurs at a frequency approximately 6.25 times that of the fundamental.<sup>21</sup> This mode and the fundamental are termed symmetric since the tines of the tuning fork both move outward or inward at the same time. There are also antisymmetric in-plane modes in which the tines move together in the same direction, i.e., both to the right or both to the left at the same time.

For the small 426.6-Hz tuning fork, the lowest frequency antisymmetric in-plane mode occurred at 275 Hz when the fork was firmly clamped at the stem. This mode cannot be modeled as a quadrupole source, since both tines are moving together with the same phase. Instead, one might try a dipole source. Even though there are two tines, this should be a valid guess since the separation of the two tines is much smaller than a wavelength.

The pressure amplitude of the sound field radiated by an acoustic dipole may be written as<sup>15</sup>

$$p(r, \theta) = \frac{A'k}{r} \cos \theta, \quad (6)$$

where  $A'$  is an amplitude factor which depends on the size, strength, and frequency of the dipole source. Figure 12(a) shows a polar plot of the directivity pattern for a dipole source. Figure 12(b) shows a frame from an animated GIF movie<sup>12</sup> which illustrates the sound field produced by a

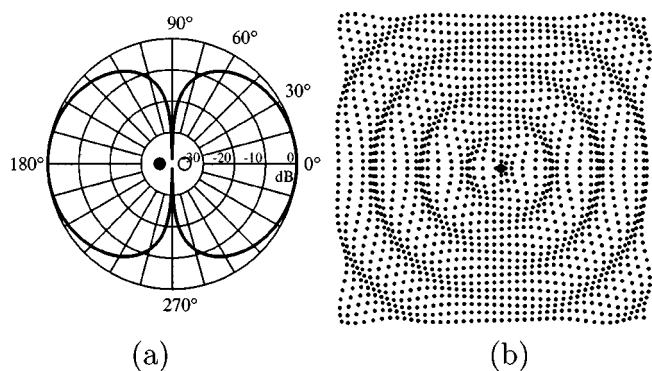


Fig. 12. (a) Directivity pattern for a dipole source. (b) Frame from a movie (Ref. 12) showing the sound field produced by a dipole source (oscillating sphere).

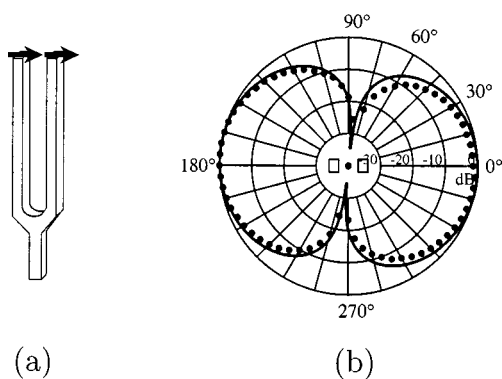


Fig. 13. 275-Hz antisymmetric in-plane mode for the small 426.6-Hz fork. (a) Relative tine motion. (b) Measured directivity pattern at a distance of 5 cm. Solid curves are for a dipole from Eq. (6).

transversely oscillating sphere. Circular wave fronts with opposite phase are propagated left and right as the sphere moves back and forth in the horizontal direction. Fluid directly above and below the sphere sloshes back and forth as the sphere oscillates, but there is no wave propagation along the vertical axis of the figure [corresponding to  $90^\circ$  and  $270^\circ$  in Fig. 12(a)].

Figure 13 shows the relative motion of the tines in the lowest antisymmetric mode and the resulting directivity pattern measured at a distance of 5 cm from the fork. The data can be rather well fit to the dipole expression in Eq. (6), thus validating our guess at modeling this vibrational mode as a dipole-type source. The measurements appear to be rotated clockwise about  $10^\circ$  from the plane of the tines; the theory fit was rotated to match the data. This is probably due to an unbalanced loading of the fork caused by the attached magnets.

In addition to the in-plane symmetric and antisymmetric modes, there are also several modes of vibration in which the motion of the tines is perpendicular to the plane of the fork. In the lowest frequency out-of-plane mode both tines move together as in Fig. 14(a). For the large 426.6-Hz tuning fork, this resonant vibration occurred at 344 Hz. The motion of the tines in this mode suggests a dipole-type behavior, as was the case for the in-plane antisymmetric mode. Figure 14(b) shows that measurements of the sound field radiated by this mode agree rather well with predicted results using the dipole expression in Eq. (6).

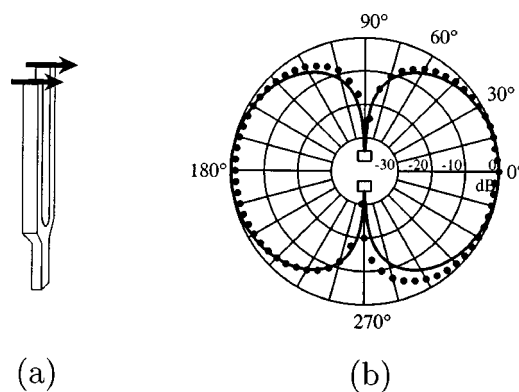


Fig. 14. 344-Hz out-of-plane mode for the large 426-Hz tuning fork. (a) Relative tine motion. (b) Measured directivity pattern at a distance of 5 cm. Solid curves are for a dipole from Eq. (6).

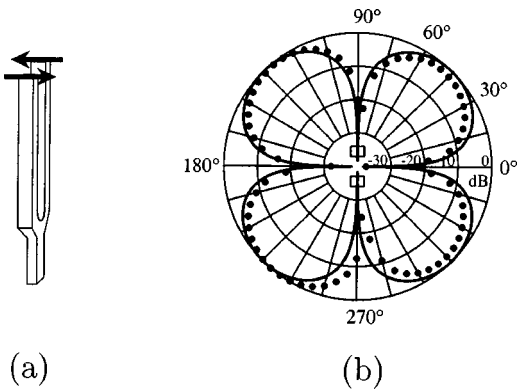


Fig. 15. 483-Hz out-of-plane mode for the large 426-Hz tuning fork. (a) Relative tine motion. (b) Measured directivity pattern at a distance of 5 cm. Solid curves are for a lateral quadrupole from Eq. (3).

If the stem of the tuning fork is rigidly clamped so that the fork cannot rotate, a more prominent mode may be found in which the tines move with opposite phase perpendicular to the plane of the fork. The frequency of this mode of vibration is usually fairly close to the fundamental frequency of the fork.<sup>4</sup> In the large 426.6-Hz fork used in this experiment this out-of-plane mode occurred at 482 Hz. Figure 15(a) shows the relative motion of the tines. This vibrational mode bears similarity to a lateral quadrupole source as described in Sec. II. As Fig. 15(b) shows, measurements of the sound field radiated by this mode agree very well with lateral quadrupole theory from Eq. (2).

## VI. OTHER OBSERVATIONS

Wood<sup>17</sup> and Rayleigh<sup>22</sup> cite a simple experiment by Stokes<sup>23</sup> in which a piece of cardboard is lined up with the fork tines. When the cardboard is held in regions A or B of Fig. 1(b), nothing happens, but when held along one of the dotted lines in Fig. 1(b), the loudness of the fork dramatically increases. The dipole motion of each tine produces circulation of air around the tine as it vibrates back and forth.<sup>6,24</sup> Placing cardboard along one of the dotted lines interrupts this circulation and destroys the dipole nature of the tine. This is akin to the increase in sound which results from placing a loudspeaker in a baffle.<sup>18</sup> Passing a tuning fork through a slot cut in a piece of cardboard produces the same effect.<sup>21,25</sup>

In a similar experiment, covering one of the tines with a cylinder dramatically increases the sound level at what was previously a minimum.<sup>1</sup> An explanation for this effect is that covering one tine changes a linear quadrupole into a dipole. Comparing Figs. 5(b) and 12(a), it is seen that the near-field directivity pattern for the dipole has a significant sound level at the location of a minimum for the linear quadrupole. The sound level in the plane of the tines will also increase because dipole sources are much more effective radiators of sound than are quadrupoles.<sup>13</sup> The radiation efficiency of a dipole varies with the fourth power of frequency whereas quadrupole radiation varies as the sixth power.

## VII. CONCLUDING REMARKS

A tuning fork vibrating in its fundamental mode of vibration is a rather complicated radiator of sound, exhibiting distinct near-field and far-field directivity patterns. Naive at-

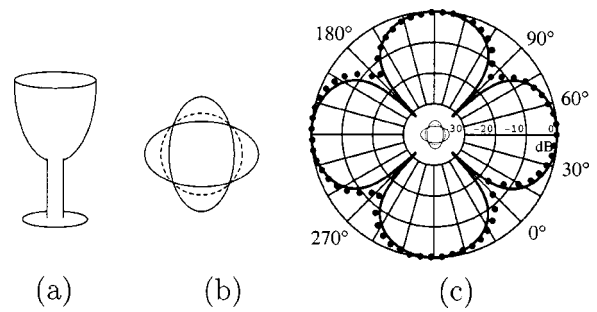


Fig. 16. (a) Wineglass. (b) Exaggerated top view of the glass vibrating in its fundamental mode. (c) Sound field measured at a distance of 20 cm from the glass fit with a lateral quadrupole directivity pattern.

tempts at explaining the radiated sound field in terms of compressions, rarefactions, and interference effects are unable to explain the details of the radiated sound field; a lateral quadrupole-type source also does not correctly model both the near- and far-field radiated patterns. A linear quadrupole model appears to correctly predict the locations and relative amplitudes of observed maxima and minima both when the fork is held close to the ear and when it is held at arm's length. Other, less commonly observed, vibrational modes behave as dipole sources, and one mode exists in which the tines move as a lateral quadrupole. The tuning fork is thus a simple device which can be effectively used to demonstrate the more advanced concept of near-field and far-field radiation as well as the behavior of a linear quadrupole acoustic source.

## APPENDIX: SOUND FIELD FROM A WINEGLASS

When a wineglass is made to vibrate in its fundamental mode, either by rubbing a wet finger around the rim or by tapping the glass with a knuckle, it vibrates in a fashion similar to what is termed the (2,0) mode of a bell.<sup>26,27</sup> The radial cross section of the glass oscillates according to Eq. (1), as shown in Fig. 2. A wine glass is thus a good example of a lateral quadrupole source. An inexpensive (\$1.95) glass was driven at its fundamental frequency of 895 Hz, using a small magnet and driving coil in the same manner as the tuning fork measurements. The resulting pressure sound field at 20 cm from the glass is shown in Fig. 16. The data fit very nicely with a lateral quadrupole directivity pattern from Eq. (2), and provide further evidence that this type of sound source does not accurately model the behavior of a tuning fork vibrating in its fundamental mode.

<sup>1</sup>H. L. F. Helmholtz, *On The Sensations of Tone* (1885 edition reprinted by Dover, New York, 1954), 2nd ed., p. 161.

<sup>2</sup>T. M. Yarwood, *Acoustics* (Macmillan, London, 1953), pp. 81, 108–110.

<sup>3</sup>F. S. Crawford, *Waves*, Berkeley Physics Course Vol. 3 (McGraw-Hill, New York, 1968), p. 532.

<sup>4</sup>J. Backus, *The Acoustical Foundations of Music* (Norton, New York, 1969), pp. 49, 67.

<sup>5</sup>R. W. B. Stephens and A. E. Bate, *Acoustics and Vibrational Physics* (Edward Arnold, London, 1966), 140 pp.

<sup>6</sup>A. Wood, *The Physics of Music* (Chapman and Hall, London, 1975), 7th ed., pp. 19 and 20, 40 and 41.

<sup>7</sup>R. M. Sillitto, "Angular distribution of the acoustic radiation from a tuning fork," *Am. J. Phys.* **34**, 639–644 (1966).

<sup>8</sup>M. Iona, "Sounds around a tuning fork. II," *Phys. Teach.* **14**, 4 (1976).

<sup>9</sup>L. Cremer, M. Heckl, and E. E. Ungar, *Structure-Borne Sound* (Springer-Verlag, Berlin, 1988), 2nd ed., 509 pp.

<sup>10</sup>MATHEMATICA 3.0, Wolfram Research, Inc., Champaign, IL, 1994.

- <sup>11</sup>V. W. Sparrow and D. A. Russell, “Animations Created in *Mathematica* for Acoustics Education,” *J. Acoust. Soc. Am.* **103**, 2987(A) (1998).
- <sup>12</sup><http://www.kettering.edu/~drussell/forkanim.html>.
- <sup>13</sup>D. A. Russell, J. P. Titlow, and Y.-J. Bommen, “Acoustic monopoles, dipoles, and quadrupoles: An experiment revisited,” *Am. J. Phys.* **67**, 660–664 (1999).
- <sup>14</sup>A. D. Pierce, *Acoustics, An Introduction to its Physical Principles and Applications* (Acoustical Society of America, New York, 1989), pp. 159–171.
- <sup>15</sup>D. D. Reynolds, *Engineering Principles of Acoustics: Noise and Vibration Control* (Allyn & Bacon, Boston, 1981), pp. 454, 572–583.
- <sup>16</sup>L. L. Beranek, *Acoustics* (Acoustical Society of America, New York, 1986), pp. 91–115.
- <sup>17</sup>A. B. Wood, *A Textbook of Sound* (MacMillan, New York, 1955), pp. 66, 233.
- <sup>18</sup>D. H. Towne, *Wave Phenomena* (Addison–Wesley, Reading, MA, 1967, reprinted by Dover, New York, 1988), pp. 205–207.
- <sup>19</sup>E. Meyer and E. G. Neumann, *Physical and Applied Acoustics: An Introduction* (Academic, New York, 1972), pp. 154–160.
- <sup>20</sup>J. B. Marion and M. A. Heald, *Classical Electromagnetic Radiation* (Harcourt–Brace–Jovanovich, New York, 1980), 2nd ed., pp. 42–47.
- <sup>21</sup>T. D. Rossing, D. A. Russell, and D. E. Brown, “On the acoustics of tuning forks,” *Am. J. Phys.* **60**, 620–626 (1992).
- <sup>22</sup>J. W. S. Rayleigh, *The Theory of Sound* (Dover, New York, 1954), Vol. 2, 2nd ed., pp. 306, 307.
- <sup>23</sup>G. G. Stokes, “On the communication of vibration from a vibrating body to a surrounding gas,” *Philos. Trans. R. Soc. London* **158**, 447–463 (1868).
- <sup>24</sup>R. H. Randall, *An Introduction to Acoustics* (Addison–Wesley, Cambridge, MA, 1951), pp. 67–69.
- <sup>25</sup>T. D. Rossing, *Science of Sound* (Addison–Wesley, New York, 1990), p. 405.
- <sup>26</sup>T. D. Rossing, “Acoustics of the glass harmonica,” *J. Acoust. Soc. Am.* **95**, 1106–1111 (1994).
- <sup>27</sup>A. P. French, “In vino veritas: A study of wineglass acoustics,” *Am. J. Phys.* **51**, 688–694 (1983).

### FERMI’S THEORY OF BETA DECAY

Emilio Segrè notes that Oppenheimer “sometimes appeared amateurish and snobbish.” Out of curiosity in 1940, while visiting Berkeley to deliver a lecture, Enrico Fermi attended a seminar one of Oppenheimer’s protégés led in the master’s style. “Emilio,” Fermi joked afterward with Segrè, “I am getting rusty and old. I cannot follow the highbrow theory developed by Oppenheimer’s pupils anymore. I went to their seminar and was depressed by my inability to understand them. Only the last sentence cheered me up; it was: ‘and this is Fermi’s theory of beta decay.’”

Richard Rhodes, *The Making of the Atomic Bomb* (Simon & Schuster, New York, 1986), p. 444.